

1 Abstract

2 Acidic Mine Waters (AMWs) are characterised by high acidity ($\text{pH} < 3$) as H_2SO_4 and elevated
3 contents of metals (Al, Fe, Cu, Zn), including rare earth elements (REEs). Due to the exhaustion
4 of minable REE containing-minerals, AMWs are increasingly regarded as an alternative source
5 of REEs. Among the different alternatives for the pre-concentration of AMWs required to make
6 the REE extraction possible, nanofiltration (NF) membranes emerge as a promising technology
7 because they not only successfully reject multivalent ions (metals), allowing its concentration
8 in the retentate stream, but also permit the transport of monovalent ones, such as H^+ and
9 HSO_4^- , allowing the recovery of sulphuric acid in the permeate. Despite this potential of NF,
10 there is still a lack of modelling tools for predicting the performance of NF membranes because
11 of its dependence on solution composition, membrane properties and interaction between
12 both. In this study, a prediction tool based on the Solution-Electro-Diffusion model (including
13 the effect of solution composition) was developed and experimentally validated for the
14 application of two polyamide-based NF membranes (NF270 and Desal DL) for the recovery of
15 REEs and H_2SO_4 from three different synthetic solutions mimicking AMWs ($\text{pH} 1.0$, 60 mg/L
16 REEs and, $25\text{-}600 \text{ mg/L}$ Al, Cu, Ca and Zn) differing in their Fe concentration ($0\text{-}2125 \text{ mg/L}$).
17 Metals were effectively rejected ($>98\%$), whereas H_2SO_4 was transported across the
18 membrane (H^+ rejections $<30\%$). The mathematical model was able to predict the
19 performance of both membranes as well as the potential scaling events associated with Fe and
20 Al hydroxides and hydroxy-sulphates.

21 **Keywords:** resource recovery; acidic mine waters; NF270; Desal DL; nanofiltration

22

1. Introduction

The European Union has identified a list of critical materials based on their high importance to its economy and the high risk associated with their supply. This list includes phosphorous, magnesium, tungsten, vanadium and rare earth elements (REEs), which comprise in turn lanthanides, scandium and yttrium, to name a few (European Commission, 2018). Because of their chemical and physical properties, REEs are widely used in electronic, optical, magnetic and nuclear applications, among others (MacLennan, 1989; Wu et al., 2018). Due to the scarcity of these critical elements, circular economy schemes are currently being proposed for their recovery from alternative sources and re-uses.

REEs are found in nature in sedimentary and igneous rocks as oxides. However, the exhaustion of these minerals has made that secondary resources such as permanent magnets, fluorescent lamps, nickel-metal hydride batteries and cathode-ray tubes from television or computer monitors are being evaluated as alternative REE sources (Binnemans et al., 2013). These solid wastes are usually leached with acids, and REE in the generated leachates can then be recovered by solvent extraction, yielding high purity REE-compounds (Jha et al., 2016; Xie et al., 2014).

Other wastes, such as acidic mine waters (AMWs), can be regarded also as REE sources, especially in Europe, which faces a shortage of REEs primary resources. Acidic mine waters (AMWs) are a by-product of the mining industry that occur when sulphide minerals, such as pyrite (FeS_2), are oxidised when entering in contact with water and oxygen. The oxidation of sulphide minerals leads to sulphuric acid production, which can dissolve the surrounding soil minerals. Then, a sulphuric-based stream containing a high content of iron, aluminium, zinc and copper, and a minor presence of REEs is released to the environment (Olías et al., 2004; Sánchez-Andrea et al., 2014; Simate and Ndlovu, 2014). One of the most known cases of AMW generation is allocated in the Iberian Pyrite Belt (South of Spain), where AMWs are

1 characterised by a pH ranging between 1 and 3.2 and a considerable amount of metals: Al, Fe,
2 Zn, Cu, and Ni, among others. Harmful elements are also present, such as As (<100 mg/L), Cd
3 (<2 mg/L), Cr (<2 ppm) and Pb (<4 ppm) and As (<10 mg/L), while REE at concentrations from
4 0.3 to 11.7 mg/L of REE (Ayora et al., 2016; Cánovas et al., 2007; Olías et al., 2016). Due to
5 their composition, AMWs can cause acute and chronic diseases in both animals and plants. In
6 animals heavy metals can accumulate in tissues and organs, disrupting their metabolic
7 functions and inhibiting the absorption of vital minerals. In plants, the presence of heavy
8 metals can cause oxidative stress that leads to cellular damage and disturbs the cellular ionic
9 homeostasis, disrupting the physiology and morphology of plants. Moreover, low pH values
10 typical of AMWs (<4.5) can also have adverse effects on many acid-sensitive aquatic organisms
11 that cannot tolerate these levels of acidity (Simate and Ndlovu, 2014). Such composition
12 makes it necessary to treat AMWs properly in order to avoid environmental issues.

13 As stated above, AMWs can be considered as an alternative source for REEs recovery.
14 However, due to the low concentration of REE in AMWs (in comparison with leachates from
15 REE-containing minerals) it is desirable to concentrate them before acid neutralisation and
16 solvent extraction steps are carried out for REE recovery. This concentration can be
17 accomplished by membrane technologies (e.g. reverse osmosis (Zhong et al., 2007), forward
18 osmosis (Qiu and He, 2019), nanofiltration (NF) (Ricci et al., 2015) or electrodialysis (Reig et al.,
19 2018)). Among these, NF membranes are gaining importance and are increasingly applied for
20 the treatment of a wide range of waters, including: brackish water (Su et al., 2017), surface
21 water (Foureaux et al., 2019) and landfill leachates (Luo et al., 2020), among others. NF
22 membranes have demonstrated to offer two-fold benefits when treating AMWs: on the one
23 hand, they can concentrate multi-charged ions (and hence REEs) in the retentate side while, on
24 the other hand, and thanks to their ability to allow permeation of mono-charged ions they can
25 concentrate, under high acidity conditions typical of AMWs, H^+ and HSO_4^- (i.e. H_2SO_4) in the
26 permeate side. This sulphuric acid stream can even be recycled and reused in leaching steps if

1 needed (Kose Mutlu et al., 2018; Mullett et al., 2014). Moreover, since one of the main issues
2 when treating AMW is its large volume needed to be treated, NF membranes can arise as an
3 effective means to reduce it by a factor from 2 to 3.

4 Nevertheless, and contrarily to reverse osmosis processes, there is still a lack of mathematical
5 models to scale and predict the behaviour of NF membranes for treating AMWs. Mathematical
6 models such as the so-called Solution-Electro-Diffusion (SED) one can describe the transport of
7 species across NF membranes using membrane permeances. This model is based on two
8 assumptions: (i) the separation is achieved due to differences in species diffusivities; and (ii)
9 membranes do not present fixed pores but have a free volume instead (Yaroshchuk et al.,
10 2011). In general, most of the efforts have so far been centred in the description of solutions
11 containing strong electrolytes where the formation of chemical species between ions in
12 solutions is not expected. However, such a scenario is only a too simple representation of real
13 AMWs, where each element may give rise to multiple species in equilibrium with each other.

14 Recent studies have included reactive transport (i.e. chemical association between species) to
15 provide a more accurate approximation (López et al., 2018b; Niewersch et al., 2014). Despite
16 these improvements in transport modelling through NF membranes, organic membrane
17 fouling and scaling events have not been taken into consideration so far on the basis of the low
18 contents of organic matter (below 5 mg/L measured as Total Organic Content), carbonate and
19 phosphate (below 1 mg/L) is relatively low. Nevertheless, special attention must be directed
20 towards the precipitation of sulphate-based minerals, especially Fe and Al hydroxy-sulphates
21 (schwertmannite ($\text{Fe}_8\text{O}_8(\text{OH})_6\text{SO}_4(\text{s})$) and basaluminite ($\text{Al}_4\text{SO}_4(\text{OH})_{10}\cdot 5\text{H}_2\text{O}$)), which can co-
22 extract REEs in solution (Lozano et al., 2020, 2019). Therefore, the potential of scaling should
23 be considered by any modelling algorithm aimed at describing transport through NF
24 membranes.

25 This work addresses the lack of modelling tools for predicting the performance of NF
26 membranes. A mathematical approach (based on SED model) is presented to predict the

1 behaviour of NF membranes when treating AMWs. Besides, the effect of solution composition
2 on membrane performance was included in the mathematical approach by empirically
3 adjusting the dependence of membrane permeances toward species on the concentration of
4 main components in solution. In order to validate the results and the model, experiments were
5 performed with two different NF membranes (NF270 and Desal DL).

6 **2. Experimental**

7 *2.1. Membranes and solutions*

8 Two commercial NF membranes were tested, namely NF270 (from Dow Chemical) and Desal
9 DL (from GE Osmonics), both with a top layer based on a semi-aromatic poly-(piperazine
10 amide). According to the manufacturers, Desal DL incorporates an additional proprietary
11 second layer made of a material comparable to a polyamide, which impacts on membrane
12 properties, such as surface roughness, hydrophilicity and acid-base properties. Both
13 membranes have ionisable amine ($R-NH_2/R-NH_3^+$) and carboxylic ($R-COOH/R-COO^-$) groups,
14 which are responsible for the membrane charge. The isoelectric points (IEPs) are 2.5 and 4.0
15 for NF270 and Desal DL, respectively (Kallioinen et al., 2016). The main properties of these
16 membranes are collected in **Table S1 (Supplementary information)**.

17 The presence of Fe (as a mixture of Fe(II) and Fe(III)) in the AMW to be treated can limit the
18 recovery options of REEs. For this reason, Fe(II) is sometimes pre-oxidized to Fe(III), which is
19 then removed by precipitation with a low-cost alkali reagent (e.g. CaO or CaCO₃).

20 Three synthetic solutions mimicking an AMW from La Poderosa Mine at the Iberian Pyrite Belt
21 (Huelva, Spain), having undergone different degrees of pre-oxidation for Fe removal, were
22 treated. All these solutions contained a sulphuric media (pH around 1.0 ± 0.1) and Al(III) (600
23 mg/L), Ca(II) and Zn(II) (40 mg/L each), Cu (25 mg/L) and REE such as La, Dy, Nd, Pr, Sm and Yb
24 (10 mg/L each one), but differed in their concentration of Fe(III), which was 0, 500 and 2125

1 mg/L. All metals (Al, Ca, Zn and Cu) were added as metal-sulphate salts, while REEs were added
2 as chlorides, nitrates, sulphates or oxides. For two solutions, iron was added to the solution as
3 Fe(II) in the form of FeSO₄, and was then oxidised with an excess of H₂O₂ (the double than the
4 stoichiometric) to convert Fe(II) into Fe(III). The following solutions and salts were used: H₂SO₄
5 (96 wt%, Sigma-Aldrich); Al₂(SO₄)₃·18 H₂O (55%, Panreac); CaSO₄·2H₂O (100%, Scharlau);
6 ZnSO₄·7H₂O (100%, Panreac); CuSO₄ (100%, Panreac); FeSO₄·7H₂O (98%, Sigma-Aldrich);
7 La₂(SO₄)₃·9H₂O (99.9%, Alfa Aesar); Pr(NO₃)₃·6H₂O (100% Fluka AG); NdCl₃·6H₂O (100%, Fluka
8 AG); SmCl₃ (100%, Fluka AG); Dy₂O₃ (99.9%, Fluka AG) and Yb₂O₃ (99.9% Fluka AG), H₂O₂ (30%,
9 Sigma-Aldrich).

10 A speciation analysis was performed before starting the experiments with the Hydra/Medusa
11 and PHREEQC code (Puigdomenech, 2001; U.S. Geological Survey, 2017). According to it,
12 metals can be present as a free ion (e.g. Al³⁺, Ca²⁺) or forming complexes with sulphate, giving
13 negatively or positively charged ions (e.g. AlSO₄⁺, Al(SO₄)₂⁻, CaHSO₄⁺) or even non-charged
14 species (e.g. CaSO₄). Complexes with other anions were found at negligible concentrations.
15 **Table S2 (Supplementary information)** collects the chemical equilibrium constants for metal –
16 sulphate complexes, which were used in mathematical modelling.

17 **Figure S1 (Supplementary information)** represents the sulphate fraction for a solution
18 mimicking the AMW at pH 1 as a function of Fe(III) concentration. It can be seen that the
19 increase of Fe(III) concentration leads to an increase of iron-sulphate complexes (i.e. FeHSO₄²⁺,
20 FeSO₄⁺ and Fe(SO₄)₂⁻), whereas the fraction of hydrogen-sulphate (HSO₄⁻) and sulphate (SO₄²⁻)
21 decrease. The other metals, as shown in **Table S2**, also form complexes with sulphate, but
22 their concentration in terms of sulphate fraction is lower than 1%, and therefore their profiles
23 are not depicted in **Figure S1**.

24

2.2. Membrane cross-flow experimental set-up

Experiments were carried out with a membrane cross-flow cell (GE SEPA™ CF II) using a flat-sheet membrane (0.014 m²). A thermostated 30 L tank was used to keep the synthetic solution to be treated at a constant temperature (25 ± 2 °C). Then, a high-pressure diaphragm pump (Hydra-Cell, USA) was used to pump the solution into the membrane cell at a prefixed flow rate and pressure. The set-up was provided with a needle and a by-pass valve to vary the cross-flow velocity (cfv) and the trans-membrane pressure (ΔP). The first one was located at the retentate stream, just at the exit from the membrane test cell, whereas the other valve was placed before the entrance of the solution into the module. At the feed and concentrate lines, two manometers were placed to monitor the pressure. Just before the discharge of the retentate to the tank, a flow-meter and a pre-filter cartridge (100 µm, polypropylene) were placed. Pipes were made of stainless steel to avoid corrosion issues. A scheme of the experimental set-up is shown in **Figure 1**.

Membranes were placed overnight in Milli-Q water to remove their conservation products. After that, deionised water flows across the test cell at 22 bar and cfv of 1 m/s (5 L/min) for 2h to compact the membrane. Samples of 30 mL of permeate were collected for measurements of the permeate flux (and,, with it, of the hydraulic permeability of the membrane) as well as the conductivity to determine when the membrane was compacted.

Before running an experiment, the membrane was compacted with the AMW at the same ΔP and cfv for 2 h. At this stage, both retentate and permeate were recycled back to the feed tank to keep the same conditions along with the membrane compaction. As in the previous case, permeate samples of 30 mL were taken and its conductivity was measured to ensure that the membrane was pressurised.

Experiments were run at a pre-fixed cfv of 0.7 m/s (3.46 L/min), and the ΔP was kept constant at 20 bar. During a filtration experiment, only retentate was recirculated back to the feed tank,

1 while permeate was continuously removed from the system. In previous studies, the effect of
2 ΔP on rejections was suited, and it was observed that at 20 bar metal rejections were high
3 (>98%), while the transport of H_2SO_4 was not impeded across the membrane (López et al.,
4 2019a). Moreover, at that ΔP concentration polarization was not observed. After collecting
5 500 mL of permeate and onwards, samples of the solution in the feed tank and permeate (30
6 mL each one) were analysed and data were represented as a function of permeate recovery,
7 defined as follows (Eq. 1) (Schäfer et al., 2005):

$$\% \text{ permeate recovery} = \frac{V_{t=0} - V_t}{V_{t=0}} \times 100 \quad (1)$$

8 Where $V_{t=0}$ (27 L) and V_t are the volumes of the feed tank solutions at the beginning of the
9 experiment and at time t, respectively.

10 The concentration factor for a given species was defined as the ratio between the
11 concentration of that species in the feed tank at time t and its initial concentration (C_t/C_0).

12 Experiments were finished when 30% of permeate recovery was achieved. Then the set-up
13 was cleaned with deionised water for 1h and 30 min at 22 bar and cfv of 1 m/s to remove any
14 impurity that might be left inside the cell.

15 All the experiments were carried out in duplicate. Samples from the feed tank and permeate
16 were analysed during the experiments with a pH-meter and a conductivity-meter as a
17 preliminary analysis to monitor the membrane performance.

18 2.3. Analytical methods

19 2.3.1. Measurement of the concentration of the elements in solution

20 In order to determine the concentration of the solution elements, samples were analysed
21 using Inductively Coupled Plasma Mass (7800 ICP-MS from Agilent Technologies) and Optical
22 Emission Spectrometer (5100 ICP-OES from Agilent Technologies). Before ICP analysis, samples

1 were previously filtered (0.2 µm) and acidified with 2% HNO₃. Samples were analysed by an
2 external laboratory.

3 2.3.2. Measurement of the acidity of the samples

4 Concerning the determination of the concentration of H⁺ with a pH-meter, it must be
5 highlighted that the analysable pH range with glass electrodes was, according to the
6 manufacturer, from 2 to 12, which implied that any measurement of pH in the range of 1 to 2
7 might have associated a high error and should be regarded as an approximation. Acidity
8 measurements by acid-base titration could not be done due to the precipitation of Fe and Al as
9 hydroxides along with the titration. Therefore, the acidity of the samples was determined with
10 a pH-meter (Crison® GLP21).

11 3. Numerical tool for prediction of the membrane performance

12 The equations presented in what follows were applied to the membrane itself (red box in **Fig.**
13 **2**), the membrane test cell (green box in **Fig. 2**) and the tank (orange box in **Fig. 2**) to predict
14 the behaviour of the experimental system.

15 The transport of ions across the NF membranes was described on the basis of the SED model,
16 which was coupled with reactive transport taking into account the chemical speciation in
17 solution. The transport of species across a NF membrane is defined as a combination of
18 diffusion and electromigration, whereas it is assumed there is no coupling between species
19 and solvent (i.e. no convective flux occurs). The model uses “virtual concentrations”, which are
20 defined as those in thermodynamic equilibrium with an infinitely small volume inside the
21 membrane. Thus, species flux is described according to **Equation 2** (Niewersch et al., 2014):

$$j_i = -P_i \cdot \left(\frac{dc_i}{dx} + c_i \cdot \frac{d(\ln \gamma_i)}{dx} + z_i \cdot c_i \cdot \frac{d\phi}{dx} \right) \quad (2)$$

1 where j_i , P_i , c_i , γ_i and z_i are the flux across the membrane, the membrane permeance, the
2 concentration, the activity coefficient and the valence charge of species i , respectively. x is the
3 dimensionless position in the membrane, and φ is the dimensionless virtual electrostatic
4 potential in the membrane.

5 The transport of any species i across the membrane must satisfy: i) chemical equilibrium
6 reactions between species, which once identified allow their flux to be solved (**Eq. 2**) for each
7 element that composes the species (e.g. equation referred to Al is a sum of the flux of Al^{3+} ,
8 AlSO_4^+ and $\text{Al}(\text{SO}_4)_2^-$) and ii) electroneutrality condition, defined as follows (**Eq. 3**) :

$$\sum_{i=1}^n (z_i \cdot c_i) = 0 \quad (3)$$

9 The membrane permeance to a given species i (P_i), which indicates the easiness of this species
10 to be transported across the membrane, is acknowledged to depend on the membrane, the
11 species properties and the composition of the solution (e.g. concentration of H^+ or Fe(III)).
12 Partition coefficients and possible changes in the chemical equilibrium constants are included
13 within the membrane permeances to ions (Yaroshchuk et al., 2011).

14 The SED model has proven to successfully describe rather complex experimental trends in NF
15 of electrolyte mixtures containing various dominant salts and trace ions. In previous studies,
16 the permeance of membranes NF270 and Desal DL towards the same solutes as the ones
17 investigated in the present study (Al, Ca, Zn, Cu, REE, SO_4) were determined under a variety of
18 pH values and Fe(III) concentrations at constant feed composition from 4 to 22 bar (these
19 values are collected in **Tables S3 and S4 Supplementary Information**). However, determined
20 membrane permeances were not constant and depended on solution composition.

21 In this work, since the permeate was continuously removed from the system while only
22 retentate was recirculated back to the feed tank, it was expected that the feed solution
23 composition changed with time and, with it, the membrane permeances towards the different

1 ions. One objective of this study was to fit permeances as a function of pH and Fe
2 concentration from values obtained in previous studies through an expression like **Equation 4**,
3 as proposed by **Bason et al. (Bason et al., 2010)** and **Yaroschuck (Yaroshchuk, 2002)**:

$$P_i = a_0 + a_1 \cdot X^{a_2} \quad (4)$$

4 where a_0 , a_1 and a_2 are fitting parameters and X is the concentration of H^+ or the one of Fe(III),
5 so that membrane permeances in this study could be predicted at any time as feed
6 composition changed with time

7 The flux of solvent across the membrane was described with the following equation (**Eq. 5**)
8 **(Schäfer et al., 2005)**:

$$J_v = k_w \cdot (\Delta P - \Delta \pi) \quad (5)$$

9 where J_v is the solvent flux across the membrane, k_w is the hydraulic permeability of the
10 membrane, ΔP and $\Delta \pi$ are the differences of pressure and osmotic pressure between feed
11 and permeate. Osmotic pressure is calculated according to the van't Hoff equation.

12 In the membrane test cell, global and component mass balances were solved to determine the
13 concentration and flow of the retentate stream (**Eqs. 6.a** and **6.b**):

$$Q_f = Q_r + Q_p \quad (6.a)$$

$$c_f \cdot Q_f = c_r \cdot Q_r + c_p \cdot Q_p \quad (6.b)$$

14 where Q and c are the flow and concentration, respectively. Subscripts f , r and p refer to the
15 feed, retentate and permeate, respectively.

16 Finally, an unsteady state mass balance is solved in the feed tank to determine how the
17 volume of the solution varied and how the different compounds were concentrated along with
18 the time (**Eqs. 7.a** and **7.b**).

$$\frac{dV}{dt} = Q_r - Q_f \quad (7.a)$$

$$\frac{d(c_{f,i} \cdot V)}{dt} = Q_r \cdot c_{r,i} - Q_f \cdot c_{f,i} \quad (7.b)$$

1 where V is the tank volume and t is the running time of the experiment.

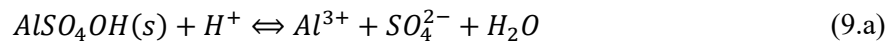
2 After solving **Equations 7.a** and **7.b**, a speciation analysis must be performed to determine the
3 composition of the different species in the feed, and then solve **Equation 2**.

4 The numerical code was implemented in Matlab to predict the performance of the system
5 (**Figure 2**).

6 Although the implemented SED model does not contemplate concentration polarisation
7 phenomenon due to the mathematical complexity of the system, the saturation indexes (SI) of
8 the potentially expected mineral phases were evaluated (**Eq. 8**) (Schäfer et al., 2005).

$$SI = \log\left(\frac{IAP}{K_{so}}\right) \quad (8)$$

9 Where K_{so} is the solubility constant and IAP is the ionic activity product of a given potential
10 mineral involved in a scaling or inorganic fouling event. For example, for the precipitation of
11 jurbanite (i.e. $AlOHSO_4$ (s)) (**Eq. 9**):



$$SI = \log\left(\frac{IAP}{K_{so}}\right) = \log\left(\frac{[Al^{3+}][SO_4^{2-}][OH^-]}{K_{so}}\right) \quad (9.b)$$

12 **Table S5 (Supplementary information)** shows a summary of the main mineral phases expected
13 to be formed in the feed solution. The commonly used software designing tools for RO
14 applications (e.g. Wave (Dow-Chem), Hydranautics, Wind-Flow (Suez)) predicts saturation
15 conditions and therefore scaling on the membranes. For such calculus, they consider

1 concentration polarisation factors. In this case, a factor of 10 was considered to assess the
2 potential fouling at the membrane.

3 **4. Results and discussion**

4 *4.1. Dependence of membrane permeances of solution composition*

5 Three different synthetic AMWs containing different concentrations of Fe (0, 500 and 2125
6 mg/L) were filtered with the NF270 and Desal DL membranes. To address the influence of
7 acidity and Fe(III) concentration on membrane permeances to each species (P_i) experimental
8 data on P_i calculated in previous studies and collected in **Supplementary information (Tables**
9 **S3 and S4)** were fitted to **Eq. 4**. P_i in the experiments without Fe(III) was expressed as a
10 function of H^+ concentration, while P_i in those containing Fe(III) was fitted as a function only of
11 Fe concentration (pH was around 1.0 ± 0.1 , and its effect on P_i was expected irrelevant
12 because membrane charge will not be modified). As an example, **Figure 3** shows the fitting of
13 NF270 membrane permeance values as a function of Fe(III) concentration. For Desal DL the
14 fitting (not shown here) was as good as the one for NF270 permeances.

15 *4.2. Prediction capabilities of the solution-electro-diffusion model in* 16 *acidic waters and validation with experimental data*

17 *4.2.1. Comparison of NF270 and Desal DL membranes for Fe(III) free acidic waters* 18 *at pH 1.0*

19 **Figure 4** shows the concentration variation of the different species in the feed tank and the
20 permeate streams when filtrating a synthetic AMW without Fe(III) at pH 1.0 for the NF270
21 (**Figs. 4.a and 4.b**) and Desal DL (**Figs. 4.c and 4.d**) membranes.

22 The results for both membranes with the solution without Fe(III) showed the potential
23 treatment capacity of AMWs with NF. Within the percentage of permeate recovery range

1 studied (0-30%), both membranes rejected metals from the feed stream at percentages higher
2 than 98% and yielded a permeate rich in sulphuric acid (6 g/L for N270 and 5 g/L for Desal DL,
3 sulphate rejections of 55% for NF270 and 69% for Desal DL) with a minor presence of metallic
4 impurities (below 5 mg/L for both membranes) (**Figure 4**). A ratio 1:1 between H⁺ and S (mainly
5 as HSO₄⁻) in the permeate was observed for both membranes, which indicated that permeate
6 was mainly composed of purified sulphuric acid. In addition, such rejection of metals (>98%)
7 made feasible concentrating REEs by a 50% at 30% of permeate recovery.
8 This similar behaviour between these two membranes could be related to the resemblance of
9 the composition of their active layers (both membranes are polyamide-based). In terms of
10 water flux across the membrane, NF270 had higher membrane permeability due to its lower
11 polyamide layer thickness (Tang et al., 2009), exhibiting then greater permeate fluxes, which is
12 in agreement with the membrane properties shown in **Table S1**. As in the previous studies,
13 NF270 and Desal DL were able to reject the metal species effectively (e.g. >98%) while they
14 allowed acid to permeate easily across the. Moreover, as in the present case, NF270 was prone
15 to transport better the acid than Desal DL.

16 These results can be explained on the basis of the main exclusion phenomena taking place in
17 NF membranes: the Donnan and dielectric exclusion. At pH 1.0, both NF270 and Desal DL
18 membranes (whose IEPs are 2.5 4.0, respectively, and thus above the pH of the feed solution)
19 are expected to be positively charged due to the partial and fully protonation of amine (R-
20 NH₃⁺) and carboxylic groups (R-COOH), respectively. This fact originates electrostatic
21 repulsions between the charged membrane surface and the metallic cations (e.g. Al³⁺, Ca²⁺,
22 Cu²⁺), which explains why these metallic cations were effectively rejected (Donnan exclusion)
23 (Yaroshchuk, 2001). Conversely, the transport of anions (e.g. HSO₄⁻) would be favoured
24 because of the electrostatic attractions between them and the positively charged membrane
25 surface. This phenomenon explained why both membranes permitted easy transport of
26 sulphate (HSO₄⁻/SO₄²⁻) through them. Nevertheless, a stoichiometric number of cations must

1 permeate to achieve electroneutrality conditions in the permeate side. Then, the H^+ was
2 transported across the membrane because of its higher diffusivity, lower size and lower
3 absolute charge than the rest of cations (Robinson and Stokes, 2002).

4 On the other hand, the dielectric exclusion must also be considered to explain the transport of
5 ions across the membrane. The cause of this phenomenon is found in the interactions that
6 arise between the ions and bound electric charges induced in the membrane at the interface
7 solution/membrane with different dielectric constants (i.e. polymeric matrix/bulk solution).
8 The effect of dielectric exclusion is more pronounced than the one of Donnan exclusion
9 because the ion-exclusion free energy is dependent on the square of the ion charge, while the
10 Donnan exclusion's is linear with it (Kim et al., 2005; Yaroshchuk, 2000). Dielectric exclusion
11 explained why the transport of multivalent metallic impurities (i.e. Al^{3+} , Ca^{2+} and Cu^{2+}) was
12 more impeded than that of H^+ .

13 Donnan and dielectric exclusion phenomena are responsible for the high selectivity of both
14 membranes for sulphate over metal ions.

15 In **Figure 4** the predicted concentration values (solid lines) were calculated by using the
16 permeances to species from **Supplementary Information (Tables S3 and S4)**. As can be seen,
17 the calculated concentration values matched the experimental values consistently in the feed
18 tank for both membranes and both dominant and minor species in solution. With regard to the
19 permeate stream, a good matching was generally obtained, although significant discrepancies
20 were observed for H^+ and Al for the NF270 membrane. The discrepancy in acidity values could
21 be due to the fact that their activity values (a_{H^+}) were determined with a pH glass electrode.

22 4.2.2. Comparison of NF270 and Desal DL membranes for acidic waters containing 23 Fe(III) at pH 1.0: influence of the Fe(III) concentration

24 The influence of the Fe(III) concentration in the metal concentration and H_2SO_4 recovery
25 factors was studied at two different levels 500 mg/L and 2125 mg/L. **Figure 5** shows the

1 evolution of the concentration of the different studied solutes in the feed tank and the
2 permeate in the presence of 500 mg/L Fe(III) in the initial solution for NF270 (Figs. 5.a and 5.b)
3 and Desal DL (Figs. 5.c and 5.d) membranes, respectively.

4 The presence of Fe(III) resulted in higher rejection percentages of sulphate across the
5 membrane (67% for NF270 and 75% for Desal DL in front of 55 % and 69% in the absence of
6 Fe). The reason for such increase lies on sulphate speciation. In fact, the increase of Fe(III)
7 concentration implied an increase of the positively-charged species FeSO_4^+ and FeHSO_4^{2+} molar
8 fractions, while a decrease of the negatively-charged species HSO_4^- and SO_4^{2-} (see Figure S1),
9 resulting in enhanced overall transport of sulphate across the membrane due to Donnan and
10 dielectric exclusion phenomena (Kim et al., 2005; Yaroshchuk, 2000). Moreover, the lower
11 presence of HSO_4^- and SO_4^{2-} led also to a lower concentration of sulphate in the permeate (see
12 Figure S1).

13 Fe(III) exhibited a similar behaviour than Al(III) (see Figures 5.a and 5.c). Both membranes
14 effectively rejected Fe(III) (>98%), and the content of metallic impurities in the permeate were
15 below 7 mg/L for NF270 and 4 mg/L for Desal DL for each metal (see Figures 5.b and 5.d).
16 Moreover, the fact that Fe(III) was present in solution did not modify the concentration factor
17 for REEs (1.5 at 30% of permeate recovery). Similarly to the previous case in the absence of
18 Fe(III), NF270 provided a permeate stream richer in sulphuric acid than Desal DL (4.5 g/L and
19 3.6 g/L H_2SO_4 , respectively), as it can be seen in Figures 5.a and 5.c. The higher concentration
20 of HSO_4^- in solution favoured the passage of H^+ across the membrane.

21 The prediction capacity of the numerical code showed similar levels of accuracy than for the
22 solution without Fe(III). The better predictions for NF270 than for Desal DL, despite their
23 similar chemical properties from the point of view of the active layer, could be associated to
24 the fact that the data set of membrane permeances for the former has been more studied
25 than that of the latter.

1 The membranes performance in filtrating acidic water with high Fe(III) contents (2125 mg/L) is
2 shown in **Figure 6**. **Fig. 6.a and 6.c** represent the concentration profile in the feed tank while
3 **Fig. 6.b and 6.c** show the concentration in the permeate, respectively.

4 The increase of Fe(III) up to 2125 mg/L led to even higher sulphate rejections (73% for NF270
5 and 84% for DL) (see **Figure 5 and 6**) for the same speciation reasons discussed above (see
6 **Figure S1**). The main impurity in the permeate was Fe(III), reaching concentrations up to 68
7 mg/L for NF270 and 25 mg/L for Desal DL, while the other metals (i.e. Al, Ca, Cu, Zn and REEs)
8 remained below 10 mg/L for both membranes. Again NF270 yielded a richer stream in H₂SO₄
9 (4.2 g/L) than Desal DL (3.5 g/L), while both membranes achieved similar metal concentration
10 factors. The prediction provided by the SED model described this increase of Fe(III) in the
11 permeate up to 20-30 mg/L Fe(III) for Desal DL while predicted values for NF270 were much
12 lower than those measured experimentally (up to 70 mg/L).

13 **Table 1** collects the permeate composition at 25% recovery for the experiments performed. As
14 can be seen, the presence of Fe(III) resulted in a hindered transport of sulphuric acid across the
15 membrane and therefore in a lower concentration of sulphuric acid in the permeate, which
16 presented increased concentration of metal impurities if compared in the absence of Fe(III).
17 On the other hand, **heavy metals were effectively removed from solution (removal**
18 **percentages mostly >98%) as it occurred in the absence of Fe(III). While these streams may**
19 **exhibit some toxicity to aquatic organisms due to their high contents of metals (for the**
20 **retentate) or low pH (for the permeate) (Simate and Ndlovu, 2014), they are not planned to be**
21 **discharged into waterbodies but to be treated instead for the recovery of metals an sulphuric**
22 **acid, respectively.**

23 Both membranes (NF270 and Desal DL) have been studied previously in the literature for
24 wastewaters treatment. Niewersch et al. (2010) studied the selectivity of Desal DL for cations
25 (Al, Fe, Cr, Cu) and phosphoric acid when filtering sewage ash eluates and observed a high

1 passage of phosphorous, while metals such as Cu were effectively rejected (>93%) at ΔP higher
2 than 17 bar for permeate recoveries ranging from 17 to 90%. This selectivity was found to be
3 dependent on effective pressure and composition of feed solution. Wadekar and Vidic (2018)
4 compared the performance of a TiO_2 ceramic (from Cerahelix) and a polymeric (NF270) NF
5 membranes for treating mine drainage from a coal mine (pH 7.8). Ranging from permeate
6 recoveries between 0 to 75% at ΔP of 35 bar, they found that NF270 rejected effectively
7 (>96%) divalent and trivalent metal ions (e.g. Al(III), Ca(II) and Mg(II), among others), whereas
8 Cl and As exhibited the lowest rejections (<10% and 20% for Cl and As, respectively). At the
9 same time, NF270 was able to recover purified water as permeate at pH 7.8. The ceramic
10 membrane showed metal rejections between 55 and 67%, with lower rejections of Cl and As
11 (<20%).

12 The conventional ex-situ treatment of AMWs relies on acid neutralisation and metal
13 precipitation by the addition of an alkali. The drawback of this treatment is the generation of a
14 voluminous sludge rich in water, with a solid content of only 2-4%, which makes necessary
15 further solid-liquid separation units (Johnson and Hallberg, 2005; Santos et al., 2004).
16 Nevertheless, in such a treatment no valorisation of the acidic stream is considered, since acid
17 is neutralised and metals are precipitated all together and not recovered. Valorisation of
18 AMWs using membrane technologies other than NF ones has also been researched. For
19 example, Martí-Calatayud et al. (2014) treated an AMW (pH 1.68, 0.02 M $Fe_2(SO_4)_3$, 0.01 M
20 Na_2SO_4) with electrodialysis and obtained a stream with a high concentration of H_2SO_4 , while
21 Fe(III) precipitated as $Fe(OH)_3$, which caused an increase in the specific energy consumption
22 from 6 to 15 kWh/kg. Amaya-Vías et al. (2019) evaluated membrane distillation with PTFE
23 membranes for the treatment of an AMW (pH 2.1, 10.5 g/L SO_4 , 0.81 g/L Mg and 0.73 g/L Fe)
24 at different temperatures (50-80 °C), obtaining high permeate fluxes (up to 16.80 L/m²h) with
25 high metal rejections (99%). Despite the good performance of these techniques from the point
26 of view of solutes recovery, it must be taken into account that the high energy requirements

1 for electrodialysis (electrical) and membrane distillation (thermal) turn both technologies
2 unsuitable for the valorisation of AMWs, making NF a very cost-effective alternative.

3 From the experimental results, it has been seen that the presence of Fe hinders the recovery
4 of purified H₂SO₄ in the NF permeate, making thus it necessary to remove all Fe(III) before the
5 NF stage. This can be achieved by Fe(III) precipitation at pH ca. 4.0 with the addition of an
6 alkali agent (e.g. caustic soda, ammonia, soda ash or hydrated lime). However, because REEs
7 can easily precipitate with basaluminite (Al₄SO₄(OH)₁₀·5H₂O) after the NF stage at pH 4.0
8 (Ayora et al., 2016), Fe(III) precipitation must be accomplished at pH<4.0. Once Fe is
9 precipitated, it would be recommended to decrease the pH down to 1.0 using, e.g. the
10 permeate rich in H₂SO₄ to ensure that NF membranes are positively charged and that they
11 effectively concentrate REE in the feed tank.

12 4.3. *Predicting the performance of NF270 and Desal DL at different* 13 *operation parameters*

14 As shown in the previous section, the model was capable of predicting the concentration in the
15 permeate and feeding tank solution within the evaluated %permeate recovery range. Because
16 of mechanical limitations of the experimental set-up, a parametric study was carried out to
17 study the effect of ΔP (10, 20, 40 and 60 bar) within a range of %permeate recovery (0-80%) on
18 metal rejection (and thus concentration factors) and sulphuric acid recovery in the permeate
19 with the composition of the solution containing 500 mg/L Fe(III).

20 **Table 2** collects the concentration factor of the elements in the feed solution (i.e. metals, REEs
21 and sulphuric acid) at the ΔP mentioned above, respectively.

22 For all the ΔP evaluated, the transport of double and triple-charged metallic cations through
23 the studied membranes was effectively hindered by Donnan and dielectric exclusion
24 phenomena, leading to higher concentration factors when %permeate recovery increased. As
25 mentioned before, the transport of HSO₄⁻ was favoured by the membrane charge at the low

1 working pH (1.0), which forced H^+ to be also transported to achieve electroneutrality
2 conditions in the permeate. As a result, a permeate rich in sulphuric acid was obtained.
3 Rejections of H^+ were around 20% lower for Desal DL than for NF270, representing a drawback
4 for the former in the recovery of sulphuric acid in the permeate. **Figure 7.a** collects the
5 sulphuric acid concentration in the permeate. NF270 would allow to obtain a higher sulphuric
6 acid concentration in the permeate than Desal DL at the same conditions (pressure,
7 %permeate recovery).

8 For example, at 10 bar and 80% of permeate recovery, acid concentration in the permeate was
9 6.6 g/L and 6.2 g/L for NF270 and Desal DL, respectively. By increasing the pressure, lower acid
10 concentration in the permeate would be achieved (**Fig. 7.a**), but the molar flux of acid
11 increased (**Fig. 7.b**).

12 Regarding the effect of ΔP on concentration factors (see **Table 2**), similar metal concentration
13 factors were achieved at all ΔP tested (10, 20, 40 and 60 bar). The only difference observed
14 between experiments run at different ΔP was that trans-membrane fluxes increased with ΔP
15 (Fig. 8.c). A comparison between membranes showed that both membranes exhibited high
16 metal rejections, leading to similar concentration factors for the different evaluated ΔP and
17 %permeate.

18 In the light of these findings, it could be anticipated that NF270 was a more suitable
19 membrane for acid recovery, especially working at ΔP of 10 bar, because H^+ permeation
20 through this membrane was higher than for the Desal DL one. At this ΔP , the low H^+ rejection
21 favoured to obtain a richer sulphuric acid permeate (6.6 g/L at 80% of permeate recovery). In
22 addition, the high metal rejections (>98%) allowed to concentrate the metals independently of
23 ΔP up to a factor of 5 at 80% permeate recovery.

24 For all the conditions evaluated, calculation of SI values for minerals with potential to cause
25 scaling and inorganic fouling (collected in **Table S5**). SI values for the mineral phases of

1 jurbanite (AlOHSO_4) and gypsum ($\text{CaSO}_4 \cdot 2\text{H}_2\text{O}$) were close to zero, indicating that their
2 precipitation on the membrane was plausible.

3 **5. Conclusions**

4 Polyamide-based NF membranes have shown their potential for their integration in the
5 treatment of AMWs since they allow the recovery of sulphuric acid as permeate and
6 concentrate the metals and REEs in the feed tank solution. The recovered sulphuric can be
7 beneficial as it can be reused on the pre-processing stages and additionally lowers the cost of
8 alkalis. Both membranes (NF270 and Desal DL) exhibited a similar behaviour due to their
9 similar active layer, but the first one is preferred since it presents higher water permeability.
10 Results showed that the electric fields originated between the membrane and dissolved
11 species govern the separation (Donnan and dielectric exclusion). Therefore, metallic ions were
12 effectively rejected by the membrane (>98%) whereas sulphuric acid was transported (H^+
13 rejections below 30%).

14 The set of membrane permeances from previous works was fitted as a function of the proton
15 and total sulphate concentration. With such expressions, it could be possible to take into
16 account the effect of solution composition within the separation.

17 Finally, a solution to the lack of NF prediction tools for the design and integration of NF
18 technology in the treatment of AMWs applications has been developed. This model can be
19 used to predict the behaviour of any effluent in continuous mode (with recirculation only of
20 the retentate) by knowing how the membrane permeances. The algorithm integrating the SED
21 model and reactive transport has proven its applicability to determine the metal concentration
22 factors and the sulphuric acid recovery at different % permeate recovery ratios. In addition,
23 the equations previously developed, allowed to take into account the effect of feed solution
24 composition in the separation process. Additionally, the prediction of the acidity and total

1 sulphate concentration are critical factors to determine the potential scaling and inorganic
2 fouling events. The use of NF membranes as a technology for liquid effluents management in
3 the mining industry could promote the reduction of the large volumes of waters that need to
4 be treated and, at the same time, be helpful in reducing the metal and non metal discharges to
5 the environment.

6 Acknowledgements

7 This research was supported by the Waste2Product project (CTM2014-57302-R) and by the
8 R2MIT project (CTM2017-85346-R) financed by the Spanish Ministry of Economy and
9 Competitiveness (MINECO) and the Catalan Government (2017-SGR-312), Spain. MINECO
10 supported the work of Julio López and Xanel Vecino within the scope of the grant (BES-2015-
11 075051) and the Juan de la Cierva contract (IJCI-2016-27445), respectively. We also want to
12 thank the contribution of Dow Chemical for the supply of the membranes; to C. Ayora (IDAEA-
13 CSIC) for AMW supply and helpful discussion on AMW treatments, to T. Susín for his help
14 during the modelling stage; to L. Vilaplana for her help during the experimental work and to A.
15 Espriu-Gascón and A. Díaz for the ICP analysis.

16 Nomenclature

a_0, a_1, a_2	Fitting parameters in Eq. 4 (-)
c	Concentration (mol/L)
IAP	Ionic activity product
j_i	Species flux across the membrane (mol/(L· $\mu\text{m/s}$))
J_v	Solvent flux across the membrane ($\mu\text{m/s}$)
$K_{T,I}$	Chemical equilibrium constant
K_{so}	Solubility constant of the mineral
k_w	Hydraulic permeability of the membrane ($\mu\text{m}/(\text{s}\cdot\text{bar})$)
P_i	Membrane permeance ($\mu\text{m/s}$)
Q	Flow (L/min)
SI	Saturation index (-)
V	Tank volume (L)
x	Dimensionless position in the membrane (-)

X	H ⁺ or Fe(III) concentration in the tank in Eq. 4 (mol/L)
z	Valence charge (-)
ΔP	Trans-membrane pressure (bar)
$\Delta\pi$	Difference of osmotic pressure across the membrane (bar)
γ	Activity coefficient (-)
φ	Dimensionless virtual electrostatic potential in the membrane (-)

1 *Subscripts*

f	Feed
i	Species i
p	Permeate
r	Retentate
t	Time

2

1 **References**

- 2 Amaya-Vías, D., Tataru, L., Herce-Sesa, B., López-López, J.A., López-Ramírez, J.A., 2019. Metals
3 removal from acid mine drainage (Tinto River, SW Spain) by water gap and air gap
4 membrane distillation. *J. Memb. Sci.* 582, 20–29.
5 <https://doi.org/10.1016/j.memsci.2019.03.081>
- 6 Ayora, C., Macías, F., Torres, E., Lozano, A., Carrero, S., Nieto, J.M., Pérez-López, R., Fernández-
7 Martínez, A., Castillo-Michel, H., 2016. Recovery of Rare Earth Elements and Yttrium from
8 Passive-Remediation Systems of Acid Mine Drainage. *Environ. Sci. Technol.* 50, 8255–
9 8262. <https://doi.org/10.1021/acs.est.6b02084>
- 10 Bason, S., Kaufman, Y., Freger, V., 2010. Analysis of Ion Transport in Nanofiltration Using
11 Phenomenological Coefficients and Structural Characteristics. *J. Phys. Chem B* 114, 3510–
12 3517. <https://doi.org/10.1021/jp911615n>
- 13 Binnemans, K., Jones, P.T., Blanpain, B., Van Gerven, T., Yang, Y., Walton, A., Buchert, M., 2013.
14 Recycling of rare earths: A critical review. *J. Clean. Prod.* 51, 1–22.
15 <https://doi.org/10.1016/j.jclepro.2012.12.037>
- 16 Cánovas, C.R., Olías, M., Nieto, J.M., Sarmiento, A.M., Cerón, J.C., 2007. Hydrogeochemical
17 characteristics of the Tinto and Odiel Rivers (SW Spain). Factors controlling metal
18 contents. *Sci. Total Environ.* 373, 363–382.
19 <https://doi.org/10.1016/j.scitotenv.2006.11.022>
- 20 Dow Chemical, C., n.d. FILMTEC NF270 Nanofiltration Elements for Commercial Systems.
- 21 European Commission, 2018. Report on Critical Raw Materials and the Circular Economy PART
22 3/3, Publications Office of the European Union.
23 <https://doi.org/10.1097/PPO.0b013e3181b9c5d5>
- 24 Foureaux, A.F.S., Reis, E.O., Lebron, Y., Moreira, V., Santos, L. V., Amaral, M.S., Lange, L.C.,

1 2019. Rejection of pharmaceutical compounds from surface water by nanofiltration and
2 reverse osmosis. *Sep. Purif. Technol.* 212, 171–179.
3 <https://doi.org/10.1016/j.seppur.2018.11.018>

4 Jha, M.K., Kumari, A., Panda, R., Rajesh Kumar, J., Yoo, K., Lee, J.Y., 2016. Review on
5 hydrometallurgical recovery of rare earth metals. *Hydrometallurgy* 165, 2–26.
6 <https://doi.org/10.1016/j.hydromet.2016.01.035>

7 Johnson, D.B., Hallberg, K.B., 2005. Acid mine drainage remediation options: a review. *Sci.*
8 *Total Environ.* 338, 3–14. <https://doi.org/10.1016/j.scitotenv.2004.09.002>

9 Kallioinen, M., Sainio, T., Lahti, J., Pihlajamäki, A., Koivikko, H., Mattila, J., Mänttari, M., 2016.
10 Effect of extended exposure to alkaline cleaning chemicals on performance of polyamide
11 (PA) nanofiltration membranes. *Sep. Purif. Technol.* 158, 115–123.
12 <https://doi.org/10.1016/j.seppur.2015.12.015>

13 Kim, S.H., Kwak, S.-Y., Suzuki, T., 2005. Evidence to demonstrate the flux-enhancement
14 mechanism in morphology-controlled thin-film-composite (TFC)membrane. *Environ. Sci.*
15 *Technol.* 39, 1764–1770.

16 Kose Mutlu, B., Cantoni, B., Turolla, A., Antonelli, M., Hsu-Kim, H., Wiesner, M.R., 2018.
17 Application of nanofiltration for Rare Earth Elements recovery from coal fly ash leachate:
18 Performance and cost evaluation. *Chem. Eng. J.* 349, 309–317.
19 <https://doi.org/10.1016/j.cej.2018.05.080>

20 López, J., Reig, M., Gibert, O., Cortina, J.L., 2019a. Recovery of sulphuric acid and added value
21 metals (Zn, Cu and rare earths) from acidic mine waters using nanofiltration membranes.
22 *Sep. Purif. Technol.* 212, 180–190. <https://doi.org/10.1016/j.seppur.2018.11.022>

23 López, J., Reig, M., Gibert, O., Cortina, J.L.L., 2019b. Integration of nanofiltration membranes in
24 recovery options of rare earth elements from acidic mine waters. *J. Clean. Prod.* 210,
25 1249–1260. <https://doi.org/10.1016/j.jclepro.2018.11.096>

1 López, J., Reig, M., Gibert, O., Torres, E., Ayora, C., Cortina, J.L., 2018a. Application of
2 nanofiltration for acidic waters containing rare earth elements: Influence of transition
3 elements, acidity and membrane stability. *Desalination* 430, 33–44.
4 <https://doi.org/10.1016/j.desal.2017.12.033>

5 López, J., Reig, M., Yaroshchuk, A., Licon, E., Gibert, O., Cortina, J.L., 2018b. Experimental and
6 theoretical study of nanofiltration of weak electrolytes: SO₄²⁻/HSO₄⁻/H⁺ system. *J.*
7 *Memb. Sci.* 550, 389–398. <https://doi.org/10.1016/j.memsci.2018.01.002>

8 Lozano, A., Ayora, C., Fernández-Martínez, A., 2020. Sorption of rare earth elements on
9 schwertmannite and their mobility in acid mine drainage treatments. *Appl. Geochemistry*
10 113, 104499. <https://doi.org/10.1016/j.apgeochem.2019.104499>

11 Lozano, A., Ayora, C., Fernández-Martínez, A., 2019. Sorption of rare earth elements onto
12 basaluminite: The role of sulfate and pH. *Geochim. Cosmochim. Acta* 258, 50–62.
13 <https://doi.org/10.1016/j.gca.2019.05.016>

14 Luo, H., Zeng, Y., Cheng, Y., He, D., Pan, X., 2020. Recent advances in municipal landfill
15 leachate: A review focusing on its characteristics, treatment, and toxicity assessment. *Sci.*
16 *Total Environ.* 703, 135468. <https://doi.org/10.1016/j.scitotenv.2019.135468>

17 MacLennan, S.M., 1989. Rare Earth Elements in sedimentary rocks: Influence of provenance
18 and sedimentary processes. B.R. Lipin G.A. McKay “Geochemistry Mineral. Rare Earth
19 *Elem. Rev. Mineral.* 169 – 200.

20 Martí-Calatayud, M.C., Buzzi, D.C., García-Gabaldón, M., Ortega, E., Bernardes, A.M., Tenório,
21 J.A.S., Pérez-Herranz, V., 2014. Sulfuric acid recovery from acid mine drainage by means
22 of electrodialysis. *Desalination* 343, 120–127.
23 <https://doi.org/10.1016/j.desal.2013.11.031>

24 Mullett, M., Fornarelli, R., Ralph, D., 2014. Nanofiltration of mine water: impact of feed pH and
25 membrane charge on resource recovery and water discharge. *Membranes (Basel)*. 4,

1 163–180. <https://doi.org/10.3390/membranes4020163>

2 Niewersch, C., Bloch, A.L.B., Yüce, S., Melin, T., Wessling, M., 2014. Nanofiltration for the
3 recovery of phosphorus — Development of a mass transport model. *Desalination* 346,
4 70–78. <https://doi.org/10.1016/j.desal.2014.05.011>

5 Niewersch, C., Meier, K., Wintgens, T., Melin, T., 2010. Selectivity of polyamide nanofiltration
6 membranes for cations and phosphoric acid. *Desalination* 250, 1021–1024.
7 <https://doi.org/10.1016/j.desal.2009.09.097>

8 Olías, M., Nieto, J.M., Pérez-López, R., Cánovas, C.R., Macías, F., Sarmiento, A.M., Galván, L.,
9 2016. Controls on acid mine water composition from the Iberian Pyrite Belt (SW Spain).
10 *Catena* 137, 12–23. <https://doi.org/10.1016/j.catena.2015.08.018>

11 Olías, M., Nieto, J.M., Sarmiento, A.M., Cerón, J.C., Cánovas, C.R., 2004. Seasonal water quality
12 variations in a river affected by acid mine drainage: The Odiel River (South West Spain).
13 *Sci. Total Environ.* 333, 267–281. <https://doi.org/10.1016/j.scitotenv.2004.05.012>

14 Puigdomenech, I., 2001. Chemical equilibrium software Hydra/Medusa.

15 Qiu, M., He, C., 2019. Efficient removal of heavy metal ions by forward osmosis membrane
16 with a polydopamine modified zeolitic imidazolate framework incorporated selective
17 layer. *J. Hazard. Mater.* 367, 339–347. <https://doi.org/10.1016/j.jhazmat.2018.12.096>

18 Reig, M., Vecino, X., Valderrama, C., Gibert, O., Cortina, J.L., 2018. Application of
19 electrodialysis for the removal of As from metallurgical process waters: Recovery of Cu
20 and Zn. *Sep. Purif. Technol.* 195, 404–412. <https://doi.org/10.1016/j.seppur.2017.12.040>

21 Ricci, B.C., Ferreira, C.D., Aguiar, A.O., Amaral, M.C.S., 2015. Integration of nanofiltration and
22 reverse osmosis for metal separation and sulfuric acid recovery from gold mining
23 effluent. *Sep. Purif. Technol.* 154, 11–21. <https://doi.org/10.1016/j.seppur.2015.08.040>

24 Robinson, R.A., Stokes, R.H., 2002. *Electrolyte Solutions*, Second Rev. ed. Dover Books on

1 Chemistry Series.

2 Saidani, H., Amar, N. Ben, Palmeri, J., Deratani, A., 2010. Interplay between the transport of
3 solutes across nanofiltration membranes and the thermal properties of the thin active
4 layer. *Langmuir* 26, 2574–2583. <https://doi.org/10.1021/la9028723>

5 Sánchez-Andrea, I., Sanz, J.L., Bijmans, M.F.M., Stams, A.J.M., 2014. Sulfate reduction at low
6 pH to remediate acid mine drainage. *J. Hazard. Mater.* 269, 98–109.
7 <https://doi.org/10.1016/j.jhazmat.2013.12.032>

8 Santos, S., Machado, R., Correia, M.J.N., Carvalho, J.R., 2004. Treatment of acid mining waters.
9 *Miner. Eng.* 17, 225–232. <https://doi.org/10.1016/j.mineng.2003.09.015>

10 Schäfer, A.I., Fane, A.G., Waite, T.D., 2005. *Nanofiltration - Principles and Applications*, Elsevier
11 L. ed.

12 Simate, G.S., Ndlovu, S., 2014. Acid mine drainage: Challenges and opportunities. *J. Environ.*
13 *Chem. Eng.* 2, 1785–1803. <https://doi.org/10.1016/j.jece.2014.07.021>

14 Su, X., Song, Y., Li, T., Gao, C., 2017. Effect of feed water characteristics on nanofiltration
15 separating performance for brackish water treatment in the Huanghuai region of China. *J.*
16 *Water Process Eng.* 19, 147–155. <https://doi.org/10.1016/j.jwpe.2017.07.021>

17 Tang, C.Y., Kwon, Y.N., Leckie, J.O., 2009. Effect of membrane chemistry and coating layer on
18 physiochemical properties of thin film composite polyamide RO and NF membranes. I.
19 FTIR and XPS characterization of polyamide and coating layer chemistry. *Desalination*
20 242, 149–167. <https://doi.org/10.1016/j.desal.2008.04.003>

21 Technologies, S.W., 2017. DL series industrial high flow nanofiltration elements [WWW
22 Document]. URL <https://www.suezwatertechnologies.com/kcpguest/documents/Fact>
23 [Sheets_Cust/Americas/English/FS1248EN.pdf](https://www.suezwatertechnologies.com/kcpguest/documents/Fact_Sheets_Cust/Americas/English/FS1248EN.pdf)

24 U.S. Geological Survey, 2017. PHREEQC Version 3.

- 1 Wadekar, S.S., Vidic, R.D., 2018. Comparison of ceramic and polymeric nanofiltration
2 membranes for treatment of abandoned coal mine drainage. *Desalination* 440, 135–145.
3 <https://doi.org/10.1016/j.desal.2018.01.008>
- 4 Wu, S., Wang, L., Zhao, L., Zhang, P., El-Shall, H., Moudgil, B., Huang, X., Zhang, L., 2018.
5 Recovery of rare earth elements from phosphate rock by hydrometallurgical processes –
6 A critical review. *Chem. Eng. J.* 335, 774–800. <https://doi.org/10.1016/j.cej.2017.10.143>
- 7 Xie, F., An, T., Dreisinger, D., Doyle, F., 2014. A critical review on solvent extraction of rare
8 earths from aqueous solutions. *Miner. Eng.* 56, 10–28.
9 <https://doi.org/10.1016/j.mineng.2013.10.021>
- 10 Yaroshchuk, A., Martínez-Lladó, X., Llenas, L., Rovira, M., de Pablo, J., 2011. Solution-diffusion-
11 film model for the description of pressure-driven trans-membrane transfer of electrolyte
12 mixtures: One dominant salt and trace ions. *J. Memb. Sci.* 368, 192–201.
13 <https://doi.org/10.1016/j.memsci.2010.11.037>
- 14 Yaroshchuk, A.A.E., 2000. Dielectric exclusion of ions from membranes. *Adv. Colloid Interface*
15 *Sci.* 85, 193–230. [https://doi.org/10.1016/S0001-8686\(99\)00021-4](https://doi.org/10.1016/S0001-8686(99)00021-4)
- 16 Yaroshchuk, A.E., 2002. Rejection of single salts versus transmembrane volume flow in RO/NF:
17 thermodynamic properties, model of constant coefficients, and its modification. *J. Memb.*
18 *Sci.* 198, 285–297. [https://doi.org/10.1016/S0376-7388\(01\)00668-8](https://doi.org/10.1016/S0376-7388(01)00668-8)
- 19 Yaroshchuk, A.E., 2001. Non-steric mechanisms of nanofiltration : superposition of Donnan and
20 dielectric exclusion. *Sep. Purif. Technol.* 22-23, 143–158.
- 21 Yu, Y., Zhao, C., Yu, L., Li, P., Wang, T., Xu, Y., 2016. Removal of perfluorooctane sulfonates
22 from water by a hybrid coagulation-nanofiltration process. *Chem. Eng. J.* 289, 7–16.
23 <https://doi.org/10.1016/j.cej.2015.12.048>
- 24 Zhong, C.-M., Xu, Z.-L., Fang, X.-H., Cheng, L., 2007. Treatment of Acid Mine Drainage (AMD) by

1 Ultra-Low-Pressure Reverse Osmosis and Nanofiltration. *Environ. Eng. Sci.* 24, 1297–
2 1306. <https://doi.org/10.1089/ees.2006.0245>

3